J. Iran. Chem. Soc., Vol. 7, Suppl., July 2010, pp. S52-S58.

JOURNAL OF THE
Iranian
Chemical Society

Sol-Gel Preparation and Characterization of Co/TiO_2 Nanoparticles: Application to the Degradation of Methyl Orange

M. Hamadanian*, A. Reisi-Vanani and A. Majedi
Department of Physical Chemistry, Faculty of Chemistry, University of Kashan, Kashan, I. R. Iran

(Received 26 December 2008, Accepted 23 April 2009)

Cobalt doped titania nanoparticles were synthesized by sol-gel method using titanium(IV) isopropoxide and cobalt nitrate as precursors. X-Ray diffraction (XRD) results showed that titania and Co/TiO_2 nanoparticles only include anatase phase. The framework substitution of Co in TiO_2 nanoparticles was established by XRD, scanning electron microscopy equipped with energy dispersive X-ray microanalysis (SEM-EDX) and Fourier transform infrared (FT-IR) techniques. Transmission electron microscopy (TEM) images confirmed the nanocrystalline nature of Co/TiO_2. The increase of cobalt doping enhanced "red-shift" in the UV-Vis absorption spectra. The dopant suppresses the growth of TiO_2 grains, agglomerates them and shifts the band absorption of TiO_2 from ultraviolet (UV) to visible region. The photocatalytic activity of samples was tested for degradation of methyl orange (MO) solutions. Although the photocatalytic activity of undoped TiO_2 was found to be higher than that of Co/TiO_2 under UV irradiation, the presence of 0.5% Co dopant in TiO_2 resulted in a catalyst with the highest activity under visible irradiation.

Keywords: Sol-gel chemistry, Photocatalytic activity, Nanostructures, Cobalt doped TiO_2, Methyl orange degradation

INTRODUCTION

Environmental cleaning using TiO_2 photocatalysts has attracted a great deal of attention due to the increase in the level of environmental pollutions in the world [1]. Among various semiconducting materials, much attention has been given to TiO_2 because of its high photocatalytic activity, high refractive index leading to a hiding power and whiteness, resistance to photocorrosion, chemical stability, low cost and non-toxicity [2,3]. For more than a decade, studies have mainly concentrated on the suspension of TiO_2 fine powder because of its higher photocatalytic activity compared to TiO_2 thin films [4]. From among the three principal crystalline forms of titania, rutile does absorb some visible light, while anatase absorbs only in the UV region. Unfortunately, rutile is not a good photocatalyst. It is also known that optimal photocatalytic efficiency is obtained with a mixture of anatase and a small percentage of rutile [5]. Titania has a large band gap (3.20 eV for anatase TiO_2) and therefore, only a small fraction of solar light can be absorbed [5]. Many attempts have been made to sensitize titanium dioxide to the whole visible region, such as doping with transition metals [6-17], transition metal ions [18-24], nonmetal atoms [14,25-26] and organic materials [27-28]. Introduction of dopants allows titania to absorb in the visible region but this does not necessarily mean that the doped catalyst has a better photocatalytic activity. When the doping level exceedsan optimal limit, which usually lies at very low dopant concentration and low visible light absorption, the dopant causes recombination of sites and has undesirable effects on photocatalysis [5].

*Corresponding author. E-mail: hamadani@kashanu.ac.ir

The sol-gel method is an attractive method for low temperature synthesis of TiO_2, and it is easier to realize metal doping [11]. Since this method is carried out in solution, this permits tailoring of certain desired structural characteristics such as compositional homogeneity, grain size, particle morphology and porosity. Preparation of transition metal doped TiO_2 nanoparticles by sol-gel method, characterization and investigation of their photocatalytic activity have been reported in recent literature [29,30]. Preparation of Co/TiO_2 nanoparticles by sol-gel method has not been widely reported in literature. In this work, preparation and characterization of pure and Co/doped TiO_2 nanoparticles is reported and photocatalytic degradation of MO under UV-Vis light is investigated.

EXPERIMENTAL

Materials and Methods

All the chemicals were purchaced from Merck and were used without any further purification. Deionized water, prepared by an ultra pure water system (Smart-2-Pure, TKA Co., Germany), was used throughout. The typical synthesis procedure of TiO_2 and Co/TiO_2 nanoparticles was adopted from reference [29] with some variations: Titanium(IV) isopropoxide (4.7 ml) was hydrolyzed using 9.0 ml glacial acetic acid at 0 ºC. To this solution, 98.8 ml deionized water was added drop-wise under vigorous stirring for 1 h, and subsequently the solution was ultrasonicated for 15 min in ice bath. Then the stirring was continued for further 4.5 h and again the solution was ultrasonicated for 15 min in ice bath until a clear solution was formed. The prepared solution was kept under dark condition for nucleation process for 24 h. It was then gelated in an oven at 70 ºC for 12 h. The gel was dried at 100 ºC and subsequently the resulting material was powdered and then calcined in a muffle furnace at 500 ºC for 2 h. The preparation of Co/TiO_2 nanoparticles was the same as that of TiO_2, except that the water used for the synthesis, 98.8 ml, contained the required amount of cobalt nitrate (corresponding to 0.05, 0.1, 0.5, 1.0, 2.0 and 5.0 mol% compared with TiO_2).

Catalyst Characterization

The XRD patterns were recorded on a Philips X'pert Pro MPD model X-ray diffractometer using Cu Kα radiation as the X-ray source. The diffractograms were recorded in the 2θ range of 10-80º. The average crystallite size of anatase phase was determined according to the Scherrer equation. The morphology and size of nanoparticles were characterized using scanning electron microscope (SEM) (Philips XL-30ESM) equipped with an energy dispersive X-ray (EDX) and transmission electron microscope (Philips EM208). The diffuse reflectance UV-Vis spectra (DRS) of the samples were recorded by an Ava Spec-2048TEC spectrometer. FT-IR spectra of the samples were recorded on a Nicolet Magna IR 550 spectrometer. The extent of MO degradation was monitored using UV-Vis spectrophotometer (Perkin Elmer Lambda2S).

Evaluation of Photocatalytic Activity of the Samples

The photocatalytic activity was tested using MO solutions. The degradation reaction was carried out in a slurry photocatalytic reactor. The photocatalytic degradation was carried out with 100 ml aqueous MO solution (10 mg l^{-1}) containing 100 mg of catalyst nanoparticles. This mixture was aerated for 30 min to reach adsorption equilibrium. Then, the mixture was placed inside the photoreactor in which the vessel was 40 cm away from the UV and 25 cm away from the visible sources of 400 W Osram lamps. The quartz vessel and the light sources were placed inside a black box to prevent UV leakage. The experiments were performed at room temperature and a pH of about 2-3. Aliquots of the mixture were taken at periodic intervals during the irradiation, and after centrifugation they were analyzed with the UV-Vis spectrophotometer.

RESULTS AND DISCUSSION

XRD Analysis

Figure 1 shows the X-ray diffraction patterns of the undoped and 0.1, 0.5, 1.0 and 5.0% cobalt doped TiO_2 samples. The nanocrystalline anatase structure was confirmed by (1 0 1), (0 0 4), (2 0 0), (1 0 5) and (2 1 1) diffraction peaks [31]. The XRD patterns of anatase have a main peak at 2θ = 25.2º corresponding to the 101 plane (JCPDS 21-1272) while the main peaks of rutile and brookite phases are at 2θ = 27.4º (110 plane) and 2θ = 30.8º (121 plane), respectively. Therefore, rutile and brookite phases have not been detected [32,33]. The XRD patterns didn't show any Co phase (even

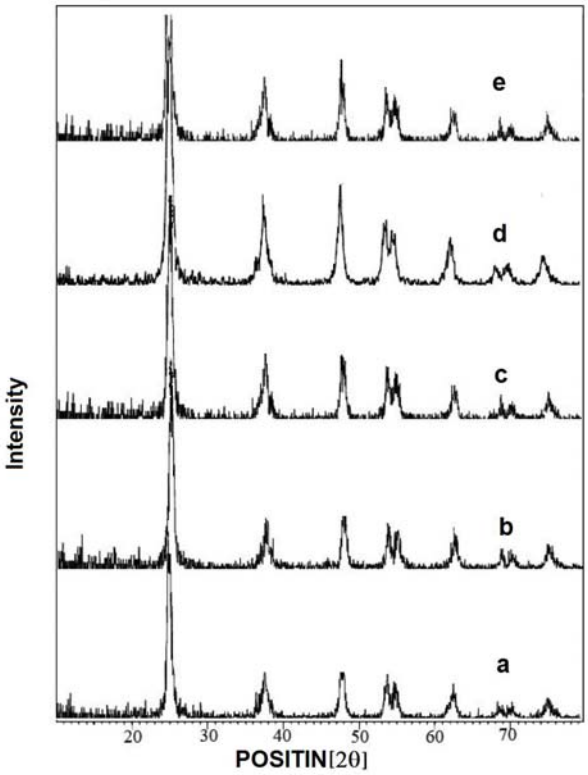

Fig. 1. XRD patterns of TiO_2 nanoparticles: (a) undoped TiO_2, (b) 0.1%, (c) 0.5%, (d) 1.0% and (e) 5.0% Co/TiO_2.

for 5% Co/TiO_2 sample) indicating that Co ions uniformly dispersed among the anatase crystallites (that was confirmed by FT-IR and SEM-EDX results, see next sections). In the region of 2θ = 10-80º, the shape of diffractive peaks of the crystal planes of pure TiO_2 is quite similar to that of Co/TiO_2 with different concentrations of Co. The average particle size was estimated from the Scherrer equation on the anatase (2θ = 25.2, 37.8, and 48.1º) diffraction peaks (the most intense peaks for each sample):

$$D = \frac{K\lambda}{\beta Cos\theta}$$

where D is the crystal size of the catalyst, λ the X-ray wavelength (1.54056 Å), β the full width at half maximum (FWHM) of the diffraction peak (radian), $K\alpha$ is a coefficient (0.89) and θ is the diffraction angle at the peak maximum. Average crystal sizes of TiO_2 and Co/TiO_2 were calculated to be around 12-14 nm and 11-13 nm, respectively. During the synthesis process, a relatively large amount of water was used to enhance the nucleophilic attack of water on titanium(IV) isopropoxide and to suppress fast condensation of titanium(IV) isopropoxide species yielding TiO_2 nanocrystals. In addition, the presence of residual alkoxy groups can significantly reduce the rate of crystallization of TiO_2 nanoparticles which favoured the formation of less dense anatase phase [34]. Furthermore, the preparation of samples was carried out in the presence of acetic acid. Since pH of solution is close to 3, there is a good chance for protonation of TiO_2 nanoparticles which could suppress further crystallization of nanoparicles. The excess acetate anion adsorbed on the surface of TiO_2 could also suppress the growth of TiO_2 nanoparticles. This type of acetate anion complexation on the surface of anatase form of TiO_2 may be the reason for the decrease of the crystallite size of TiO_2 in the sol-gel process. The addition of acetic acid did not cause residual impurities on the surface of TiO_2 after calcination, which was further confirmed by FT-IR spectroscopy (section FT-IR spectroscopy).

Scanning Electron Microscopy (SEM) and EDX Analysis

SEM micrograph of the calcined (500 ºC) pure TiO_2 nanoparticles is shown in Fig. 2. This image shows global and uniform particles which are coherent together. The EDX data of Co/TiO_2 in Fig. 3 shows two peaks around 0.2 and 4.5 keV. The intense peak is assigned to the bulk TiO_2 and the less intense one to the surface TiO_2. The peaks of Co are distinct in Fig. 3 at 0.6, 6.9 and 7.5 keV. The less intense peak is assigned to Co in the TiO_2 lattices [21]. These results confirmed the existence of Co atoms in the solid catalysts but the XRD patterns do not show any peaks related to Co (even for 5.0% Co-doped TiO_2 catalyst). Therefore, it may be concluded that Co ions are uniformly dispersed among the anatase crystallites.

Transmission Electron Microscopy (TEM)

Figure 4 shows TEM image of samples from which the particle sizes of undoped and cobalt-doped TiO_2 were found to be around 10-15 and 8-13 nm, respectively. Hence, it can be concluded that the addition of Co to titania hinders the growth

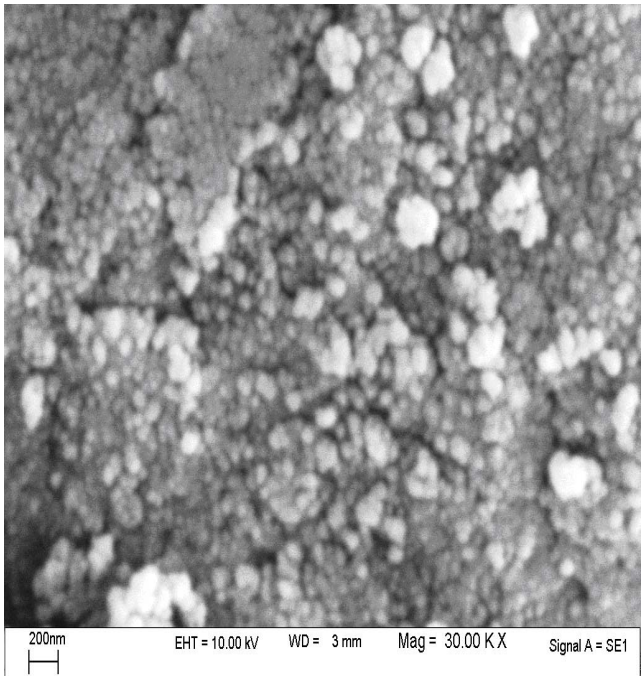

Fig. 2. SEM image of undoped TiO_2 nanoparticles.

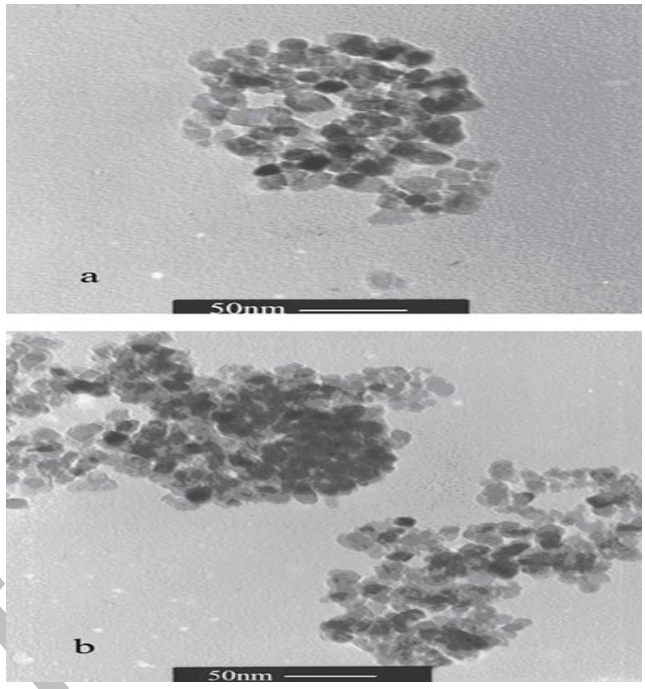

Fig. 4. TEM images of TiO_2 nanoparticles: (a) undoped TiO_2 and (b) 1.0% Co/TiO_2.

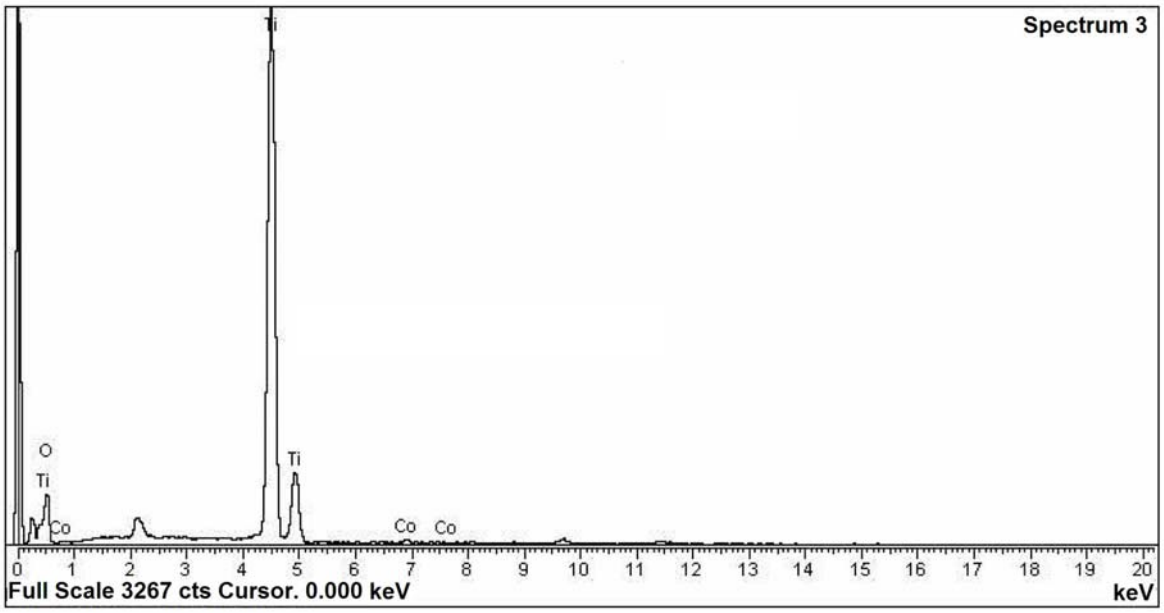

Fig. 3. EDX pattern of 0.5% Co/TiO_2 nanoparticles.

of TiO_2 nanoparticles. It seems that Co ions form complex with the TiO_2 surface oxygens, hence, suppress the growth of TiO_2 crystallite.

FT-IR Spectroscopy

FT-IR spectra of undoped and 0.5, 1.0 and 5.0% Co-doped TiO_2 samples (Fig. 5) show peaks corresponding to stretching vibrations of the O-H and bending vibrations of the adsorbed water molecules around 3350-3450 cm^{-1} and 1620-1635 cm^{-1}, respectively. The intensity of these peaks decreases with the increase in calcination temperature which indicates the removal of a large portion of the adsorbed water from TiO_2 (not shown in the figure) [20,34]. The broad intense band below 1200 cm^{-1} is due to Ti-O-Ti vibrations. The shift to the lower wavenumbers and sharpening of the Ti-O-Ti band from "a" to "d" in Fig. 5 may be due to decrease in size of the catalyst nanoparticles with increasing Co loading from 0% to 0.5%, 1.0% and 5.0%, respectively. In addition, the surface hydroxyl groups in TiO_2 increase with the increase of Co loading, which is confirmed by increase in intensity of the corresponding peaks. There is no band centered at 1389 cm^{-1} due to the bending vibrations of the C-H bond in the catalysts [35]. Also, there are no excess bands assigned for the alkoxy groups. Therefore, addition of acetic acid did not cause any residual impurities on TiO_2 surface after calcination.

UV-Vis Diffuse Reflectance Spectroscopy (DRS)

The electronic bands of the different titania samples were studied whose corresponding spectra are provided in Fig. 6.

The absorption spectrum of TiO_2 consists of a single broad intense absorption around 400 nm due to the charge-transfer from the valence band (mainly formed by 2p orbitals of the oxide anions) to the conduction band (mainly formed by 3d t_2g orbitals of the Ti^{4+} cations) [29]. The undoped TiO_2 showed absorbance in the shorter wavelength region while Co/TiO_2 and the DRS results showed a red shift in the absorption onset value in the case of Co added titania. The doping of various transitional metal ions into TiO_2 could shift its optical absorption edge from UV into visible light range, but no prominent change in TiO_2 band gap was observed [36].

Photocatalytic Activity

Degradation of MO under UV and visible irradiation was

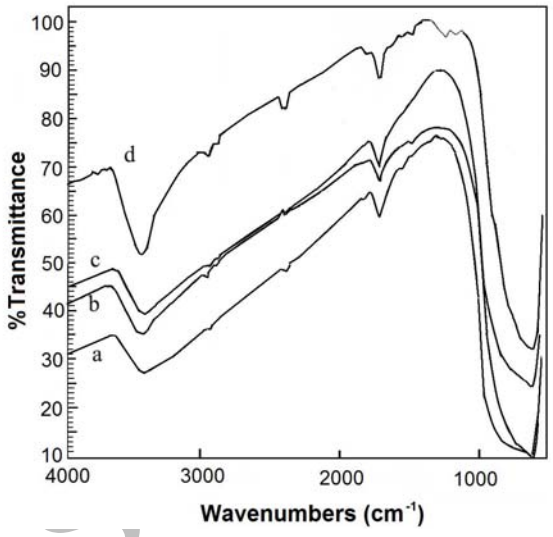

Fig. 5. FT-IR spectra of TiO_2 nanoparticles: (a) undoped TiO_2, (b) 0.5%, (c) 1.0%, and (d) 5.0% Co/TiO_2.

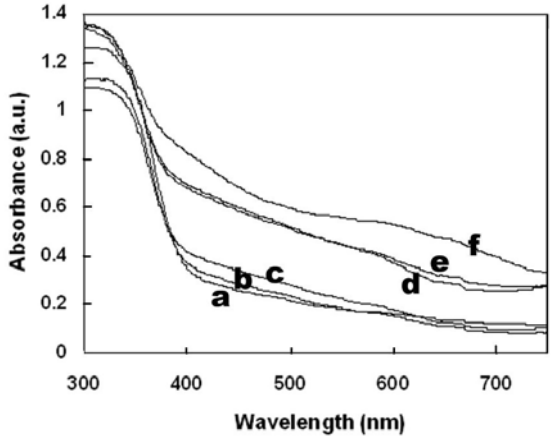

Fig. 6. DRS image of TiO_2 nanoparticles: (a) undoped TiO_2, (b) 0.05%, (c) 0.1%, (d) 0.5%, (e) 1.0% and (f) 5.0% Co/TiO_2.

followed by UV-Vis spectroscopy and the results are depicted in Figs. 7 and 8. It can be seen that under UV irradiation, undoped TiO_2 shows better results than Co/TiO_2. It seems that among the Co-doped catalysts, 1% Co/TiO_2 has the best performance. It was also observed that undoped TiO_2 decomposes MO at ~75 min while the 1.0% Co/TiO_2 does it at ~90 min. Under visible irradiation, the best degradation of MO was achieved in the presence of 0.5% Co/TiO_2, which

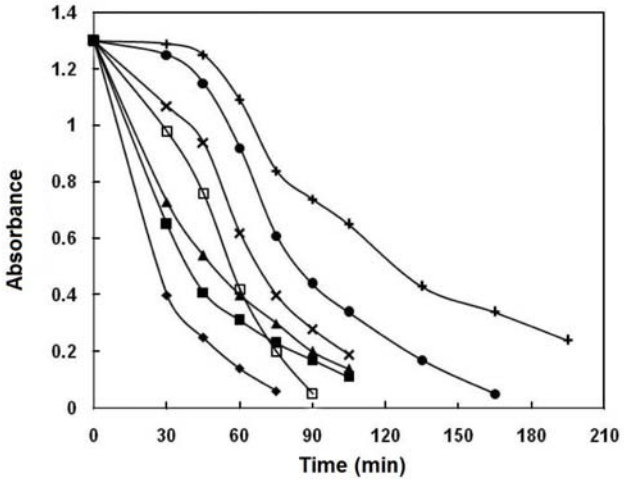

Fig. 7. Comparison of photocatalytic mineralization of MO in the presence of TiO_2 and Co/TiO_2 nanoparticles under UV irradiation. Initial concentration of MO, 10 mg l^{-1}; volume, 100 ml; pH, 2-3; catalyst dosage, 100 mg.

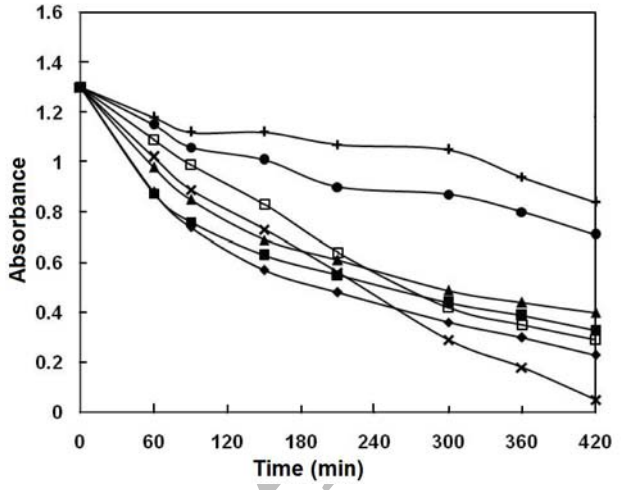

Fig. 8. Comparison of photocatalytic mineralization of MO in the presence of TiO_2 and Co/TiO_2 nanoparticles under visible irradiation. Conditions same as Fig. 7.

decomposed MO in ~420 min. In both cases (UV-Vis) the worst results were attained for the catalysts with high dopant concentrations, *i.e.*, 5.0% and 2.0% Co/TiO_2. The two basic factors that are responsible for the activity of photocatalysts include surface area and light absorption capacity.

The DRS data in Fig. 6 show that light absorption capacities of the catalysts are different and increase with an increase in the Co concentration in visible region. On the other hand, it was observed that (not shown in the figures) at relatively high Co concentrations, nanoparticles agglomerated which resulted in decreased surface area and the corresponding photocatalytic activity. Therefore, increasing the dopant concentration has two opposite effects on the photocatalytic activity of the Co/TiO_2 catalysts; increasing light absorption capacity and decreasing surface area. The photocatalytic activity depends on which one of these is the dominant factor. A lesser amount of surface hydroxyl groups was observed in the case of Co-doped TiO_2 compared with the undoped TiO_2. This could be one of the reasons for the lower activity of the metal-doped TiO_2 catalysts. Most of the metal doped TiO_2 samples absorb in the visible region. However, an investigation of the photocatalytic activity of the catalysts demonstrated that there was no direct correlation between the light absorption capacity of the Co-doped catalysts and the rate of MO degradation. It should be noted that the degradation rates in the presence of Co-doped TiO_2 catalysts under UV were in general less than that of the undoped TiO_2.

Recombination of photogenerated electrons and holes is one of the most significant factors that deteriorate the photoactivity of the TiO_2 catalyst. Any factor that suppresses the electron-hole recombination will therefore enhance the photocatalytic activity [37,38]. Perhaps, Co particles are sites for recombination of the generated electron-holes and hence, decrease the photocatalytic activity.

CONCLUSIONS

TiO_2 and Co/TiO_2 nanoparticles were prepared by the sol-gel method with sonication. From among all of the samples only anatase phase was confirmed from the XRD results. From the XRD, SEM-EDX, UV-Vis and FT-IR results, it was confirmed that the incorporation of Co in TiO_2 decreases the grain size, shifts the absorption to higher wavelenghts (red shift) and lowers the surface area due to agglomeration of the particles. The photocatalytic degradation of MO under UV irradiation revealed higher activity in the presence of the undoped than the Co-doped TiO_2. Among the Co-doped samples, the 1.0% Co/TiO_2 catalyst exhibited the highest photocatalytic activity, while under visible irradiation, the best catalyst was the 0.5% Co/TiO_2.

ACKNOWLEDGEMENTS

The authors would like to thank Dr. Nima Taghavinia of Sharif University of Technology for preparing the DRS spectra of the samples and Dr. Gholamreza Vatankhah from Art University of Isfahan for reading and editing the manuscript.

REFERENCES

[1] F.A. Fujishima, T.N. Rao, D.A. Tryk, J. Photochem. Photobiol. C 1 (2000) 1.
[2] O. Legrini, E. Oliveros, A.M. Braun, Chem. Rev. 93 (1993) 671.
[3] T. Sugimoto, X. Zhou, A. Muramatsu, J. Colloid Interface Sci. 259 (2003) 43.
[4] Y. Jiaguo, C.Y.U. Jimmy, B. Cheng, X. Zhao, J. Sol-Gel Sci. Tech. 24 (2002) 39.
[5] P. Bouras, E. Stathatos, P. Lianos, Appl. Catal. B: Environ. 73 (2007) 51.
[6] F. Sayilkan, M. Asilturk, P. Tatar, N. Kiraz, S. Sener, E. Arpac, H. Sayilkan, Mat. Res. Bull. 43 (2008) 127.
[7] J. Liqiang, S. Xiaojun, X. Baifu, W. Baiqi, C. Weimin, F. Honggang, J. Solid State Chem. 177 (2004) 3375.
[8] M. Kang, J. Mol. Catal. A 197 (2003) 173.
[9] B.Y. Lee, S.H. Park, M. Kang, S.C. Lee, S.J. Choung, Appl. Catal. A 73 (2003) 51.
[10] M.K. Seery, R. George, P. Floris, S.C. Pillai, J. Photochem. Photobio. A 189 (2007) 258.
[11] J. Zhou, Y. Zhang, X.S. Zhao, A.K. Ray, Ind. Eng. Chem. Res. 45 (2006) 3503.
[12] S.S. Lee, H.J. Kim, K.T. Jung, H.S. Kim, Y.G. Shul, Korean J. Chem. Eng. 18 (2001) 914.
[13] N. Sobana, M. Muruganadham, M. Swaminathan, J. Mol. Catal. A 258 (2006) 124.
[14] J.C.S. Wu, C.H. Chen, J. Photochem. Photobio. A 163 (2004) 509.
[15] M. Subramanian, S. Vijayalakshmi, S. Venkataraj, R. Jayavel, Thin Solid Films 516 (2008) 3776.
[16] Y. Yang, X. Li, J. Chen, L. Wang, J. Photochem. Photobio. A 163 (2004) 517.
[17] J. Lee, W. Choi, Environ. Sci. Technol. 38 (2004) 4026.
[18] S. Kim, S. Hwang, W. Choi, J. Phys. Chem. B 109 (2005) 24260.
[19] Y. Wang, H. Cheng, L. Zhang, Y. Hao, J. Ma, B. Xu, W. Li, J. Mol. Catal. A 151 (1999) 205.
[20] W. Hung, S. Fu, J. Tseng, H. Chu, T. Ko, Chemosphere 66 (2007) 2142.
[21] N. Venkatachalam, M. Palanichamy, B. Arabindoo, V. Murugesan, J. Mol. Catal. A 266 (2007) 158.
[22] J. Zhou, M. Takeuchi, A.K. Ray, M. Anpo, X.S. Zhao, Coll. Inter. Sci. 311 (2007) 497.
[23] Y. Zhang, H. Zhang, Y. Xu, Y. Wang, J. Mater. Chem. 13 (2003) 2261.
[24] J. Chen, M. Yao, X. Wang, J. Nanopart. Res. 10 (2008) 163.
[25] S. Liu, X. Chen. J. Hazard. Mater. 152 (2008) 48.
[26] M. Crisan, A. Braileanu, M. Raileanu, M. Zaharescu, D. Crisan, N. Dragan, M. Anastasescu, A. Ianculescu, I. Nitoi, V.E. Marinescu, S.M. Hodorogea, J. Non-Crystal. Solid 354 (2008) 705.
[27] D. Jiang, Y. Xu, B. Hou, D. Wu, Y. Sun, J. Solid State Chem. 180 (2007) 1787.
[28] R.S. Sonawane, B.B. Kale, M.K. Dongare, Mater. Chem. Phys. 85 (2004) 52.
[29] N. Venkatachalam, M. Palanichamy, V. Murugesan, J. Mol. Catal. A 273 (2007) 177.
[30] H. Luo, C. Wang, Y. Yan, Chem. Mater. 15 (2003) 3841.
[31] H. Ogawa, A. Abe, J. Electrochem. Soc. 128 (1981) 685.
[32] K.V. Baiju, P. Shajesh, W. Wunderlich, P. Mukundan, S.R. Kumar, K.G.K. Warrier, J. Mol. Catal. A 276 (2007) 41.
[33] K.M.K. Srivatsa, M. Bera, A. Basu, Thin Solid Films 516 (2008) 7443.
[34] N. Venkatachalam, M. Palanichamy, V. Murugesan, Mater. Chem. Phys. 104 (2007) 454.
[35] J.A. Wang, R. Limas-Ballesteros, T. Lopez, A. Moreno, R. Gomez, O. Novaro, X. Bokhimi, J. Phys. Chem. B 105 (2001) 9692.
[36] J.C.S. Wu, C.H. Chen, J. Photochem. Photobiol. A 163 (2004) 509.
[37] S. Sakthivel, M.V. Shankar, M. Palanichamy, B. Arabindoo, D.W. Bahnemann, V. Murugesan, Water Res. 38 (2004) 3001.
[38] K. Nagaveni, M.S. Hegde, G. Madras, J. Phys. Chem. B 108 (2004) 20204.